

# Quantitative dilatometric analysis of intercritical annealing in a low-silicon TRIP steel

L. ZHAO

Netherlands Institute for Metals Research, P.O. Box 5008, 2600 GA Delft, The Netherlands;  
Laboratory for Materials Science, Delft University of Technology, Rotterdamseweg 137, 2628  
AL Delft, The Netherlands  
E-mail: L.Zhao@tnw.tudelft.nl

T. A. KOP\*

Laboratory for Materials Science, Delft University of Technology, Rotterdamseweg 137, 2628  
AL Delft, The Netherlands

V. ROLIN

Université catholique de Louvain, Département des sciences des matériaux et des procédés,  
PCIM, Place Sainte-Barbe 2, B-1348 Louvain-la-Neuve, Belgium

J. SIETSMA

Laboratory for Materials Science, Delft University of Technology, Rotterdamseweg 137, 2628  
AL Delft, The Netherlands

A. MERTENS, P. J. JACQUES

Université catholique de Louvain, Département des sciences des matériaux et des procédés,  
PCIM, Place Sainte-Barbe 2, B-1348 Louvain-la-Neuve, Belgium

S. VAN DER ZWAAG

Netherlands Institute for Metals Research, P.O. Box 5008, 2600 GA Delft, The Netherlands;  
Laboratory for Materials Science, Delft University of Technology, Rotterdamseweg 137, 2628  
AL Delft, The Netherlands

---

In this work, an evaluation method to calculate the austenite fraction during continuous heating and isothermal annealing from dilatometric data is proposed. By means of a single reference measurement to determine a scaling factor correcting for experimental errors, a framework is created to determine the austenite fraction as a function of time and temperature. In the evaluation of the dilatometric data the effect of the changing carbon concentration in austenite phase is taken into account. The method is applied to dilatometric data for a 0.16C-1.5Mn-0.4Si (wt%) low-silicon transformation induced plasticity (TRIP) multiphase steel. Three typical dilatometric data are obtained by heating the material to 750°C, 800°C or 900°C, which leads to three different microstructures consisting of (1) ferrite, cementite and austenite, (2) ferrite and austenite and (3) full austenite, respectively. The calculated results using the proposed new method are compared with the results from thermodynamic analysis and those from quantitative microscopic analysis. Significant inter-test discrepancies are observed.

© 2002 Kluwer Academic Publishers

---

## 1. Introduction

During the last decade transformation induced plasticity (TRIP) multiphase steels have been significantly developed in terms of their high strength and enhanced formability. With respect to the heat treatment of TRIP steels, it has been found that the intercritical annealing condition influences the final TRIP properties, mainly the tensile strength and uniform elongation. Sakuma *et al.* [1] found that a lower temperature, just above the  $A_{c1}$  temperature, would lead to the best combination

of strength and ductility. On the other hand, Chen *et al.* [2] preferred an intermediate temperature between  $A_{c1}$  and  $A_{c3}$ , as is likely,  $(A_{c1} + A_{c3})/2$ . It was also suggested that slow cooling from an intercritical annealing temperature near the  $A_{c3}$  temperature to a temperature close to the  $A_{c1}$  temperature before rapid cooling could lead to a better balance of strength and ductility [3]. These different schedules suggested that it is desirable to improve the insight in the factors governing the phase transformation by developing a fast

\* Present Address: Philips Research, Prof. Holstlaan 4 (WA12), 5656 AA Eindhoven, The Netherlands.

and reliable method to evaluate the austenite fraction change.

The methods to evaluate the austenite fraction for TRIP steels include microscopic observations of martensite in interruptedly quenched samples [4] and thermodynamic analysis [5]. In the first method there is the possibility of the transformation of austenite to ferrite or bainite, rather than martensite, during cooling. This is more likely after intercritical annealing than after full austenitization, since the incubation time for pearlite or bainite formation is shorter due to smaller austenite grain size and no ferrite nucleation being required. The second method, thermodynamic analysis, only gives a reference for the design of the heat treatment schedule, but it is clearly incapable of taking kinetics effects into account.

As compared to these two methods, dilatometric data describe *in situ* volume fraction change during intercritical annealing, since dilatometry permits the real-time monitoring of the extent of reaction in terms of dimensional changes resulting from the phase transformations. As for the research on TRIP steels, dilatometry has been used for the determination of transformation temperatures [5–7], which showed a good reproducibility. However, no work on the evaluation method calculating austenite fraction from dilatometric data during continuous heating and subsequent intercritical annealing has been published. This is perhaps due to the difficulties dealing with an incomplete transformation of ferrite and cementite to austenite during intercritical annealing, which contains two steps: a continuous transformation during heating to above the  $Ac_1$  temperature and an isothermal transformation during holding. Therefore, the present work aims to develop and validate a suitable evaluation method for dilatometric data on an incomplete transformation. The obtained fractions will be compared with fractions deduced by two other methods, viz. quantitative scanning electron microscopy on interruptedly quenched samples and thermodynamic calculations.

## 2. Background and theoretical consideration

Dilatometry is regarded as a powerful technique for the study of phase transformations in steels, since density change resulting from phase transformation gives rise to an observable dilatation different from the thermal expansion effect. Methods to calculate this change based on the volumes of the unit cells of constituting phases have been described in literature [8–14]. Under the assumption of isotropic dilatation behaviour, the volume change ( $\Delta V = V - V_0$ ) with respect to the initial volume ( $V_0$ ) is related to the relative length change ( $\Delta l/l_0$ ) by:

$$\frac{\Delta V}{V_0} = \left(1 + \frac{\Delta l}{l_0}\right)^3 - 1 \approx \frac{3\Delta l}{l_0}. \quad (1)$$

Since the value of ( $\Delta l/l_0$ ) is very small, the square and cubic terms of  $\Delta l/l_0$  can be neglected. The right-hand side term in the equation above,  $3\Delta l/l_0$ , can be directly measured by dilatometry, while the left-hand side term,  $\Delta V/V_0$ , represents the volume change, which can be calculated based on the lattice parameters of the exist-

ing phases and is directly related to the fraction change. The influence of experimental errors, leading to deviations between calculated and measured length change is accounted for via the scaling factor  $\kappa$  [10], defined by

$$V = \kappa \cdot V_0 \cdot \left(\frac{3\Delta l}{l_0} + 1\right). \quad (2)$$

The scaling factor in the intercritical region is assumed to be proportional to the phase fractions according to

$$\kappa = (1 - f^\gamma)\kappa^\alpha + f^\gamma\kappa^\gamma, \quad (3)$$

where  $\kappa^\alpha$  and  $\kappa^\gamma$  are calculated at the  $Ac_1$  and  $Ac_3$  temperature by combining the calculated volume with the measured  $\Delta l/l_0$ . In the case of intercritical annealing of TRIP steels, three phases, ferrite ( $\alpha$ ), cementite ( $\theta$ ) and austenite ( $\gamma$ ), are involved. The lattice parameter of ferrite ( $a^\alpha$ ) is often regarded as only depending on the temperature ( $T$ ) and the expansion coefficient ( $e^\alpha$ ) [15], according to

$$a^\alpha = a_0^\alpha [1 + e^\alpha(T - T_0)], \quad (4)$$

where  $a_0^\alpha$  is the lattice parameter at the reference temperature  $T_0$ . For cementite, which has an orthorhombic structure with lattice parameters  $a^\theta$ ,  $b^\theta$ ,  $c^\theta$ , the relation is similar [15, 16]. The lattice parameter of austenite ( $a^\gamma$ ), however, is closely related to the alloying element concentrations ( $C^i$ , in wt%), in addition to the temperature and the expansion coefficient [12, 14, 17–22]. This can be expressed as follows:

$$a^\gamma = \left(a_0^\gamma + \sum_i x^i C^i\right) [1 + e^\gamma(T - T_0)], \quad (5)$$

where  $x^i$  is the coefficient relating the effect of the concentration  $C^i$  of alloying element  $i$  to the austenite lattice parameter.  $a_0^\gamma$  is the lattice parameter in unalloyed austenite at  $T_0$ . From the published  $x^i$  values [12, 14, 18], one can see that the interstitial element carbon plays a dominant role in the value of the lattice parameter of austenite, in comparison to substitutional alloying elements. For instance,  $x^i$  is zero for silicon and that for manganese is only 3% of the one for carbon [18]. Therefore, only the role of carbon is considered in the present case.

From the lattice parameters, one can easily obtain the atomic volume  $V$  of each phase in the steels. Namely,  $V^\alpha = (a^\alpha)^3/2$ ,  $V^\gamma = (a^\gamma)^3/4$ ,  $V^\theta = (a^\theta b^\theta c^\theta)/12$ , where the factors 2, 4 and 12 in the denominator arise from the fact that the unit cells of ferrite, austenite and cementite contain 2, 4 and 12 iron atoms, respectively. Considering that both the total atomic volume  $V$  and the mean carbon concentration in the material  $C_0$  follow the volume fraction rule ( $V = f^\alpha V^\alpha + f^\gamma V^\gamma + f^\theta V^\theta$ ,  $C_0 = f^\alpha C^\alpha + f^\gamma C^\gamma + f^\theta C^\theta$ ), the fractions of each phase can, in principle, be calculated from Equation 2. However, in case of the  $\alpha + \gamma$  two-phase region  $C^\gamma$  is not a constant, but depends on the fraction in a way defined by the equilibrium line in the phase diagram. Hence an analytical solution for the Equation 2 does not exist.

Nevertheless, the numerical solution for the volume fraction can be readily found using an iterative method. In the present case, the Newton-Raphson method is used because of its simplicity and great speed [23]. Carbon concentration in austenite can be accordingly calculated when the fraction is known.

In case of a multi-component structure, it is well known that the  $Ae_1$  line in the Fe-Fe<sub>3</sub>C equilibrium phase diagram is modified by the addition of alloying elements. This modification results in a three phase ( $\alpha$ ,  $\theta$  and  $\gamma$ ) co-existence region between the  $Ac_1$  and the  $Ac'_1$  temperature, a temperature at which the cementite is completely dissolved. In this three-phase region, one can assume the carbon concentration in austenite ( $C^\gamma$ ) to be nearly constant and equal to the eutectoid composition. Therefore, the following relation can be analytically derived from Equation 2:

$$f^\gamma = \frac{\kappa^\alpha V_0(3\Delta l/l_0 + 1) - k_2 V^\alpha - (1 - k_2)V^\theta}{V^\gamma - k_1 V^\alpha - (1 - k_1)V^\theta - (\kappa^\gamma - \kappa^\alpha)V_0(3\Delta l/l_0 + 1)} \quad (6)$$

$$\text{where } k_1 = \frac{C^\theta - C^\gamma}{C^\theta - C^\alpha}; \quad k_2 = \frac{C^\theta - C_0}{C^\theta - C^\alpha}.$$

One can see that the constants  $k_1$  and  $k_2$  coincide with the equilibrium volume fractions of ferrite at the eutectoid composition (pearlite) and at the nominal composition ( $C_0$ ), respectively. It is clear from the equation that the resulting austenite fraction depends on the values used for the lattice parameters of the phases involved.

### 3. Experimental

A 0.16C-1.5Mn-0.4Si (wt%) low silicon TRIP multi-phase steel was used in this investigation. The composition of silicon in this alloy is close to the lowest possible addition for significant TRIP properties [24]. The hot-rolled material was machined to a cylinder of  $\phi 4 \text{ mm} \times 10 \text{ mm}$  and the dilatometry experiments were performed on a Bähr 805 dilatometer. In the experiments, the samples were heated with a heating rate of 100°C/min to 750°C, 800°C or 900°C, respectively, isothermally held for 10 min, and quenched to room temperature. These three annealing temperatures represent three different microstructures during continuous heating: at 750°C, three phases, austenite, ferrite and cementite, co-exist, 800°C is in the intercritical region where austenite and ferrite exist and 900°C is in the fully austenitic region. Two S-type thermocouples were spot-welded on the surface of the sample to control the heating power and to record the temperature homogeneity.

The cross-section of quenched samples for the scanning electron microscopy (SEM) observations were first tempered for 2 hours at 200°C and then etched with 2% nital for 13 seconds to get a better contrast [25]. The image was analyzed using a software package named Visilog and the austenite fraction was averaged over the results from at least 25 different surface areas to reduce the influence of inhomogeneity of the phase distribu-

tion. The thermodynamic analysis was performed using the MTDData software package with a temperature interval of 1°C in the calculations. Programs to calculate the austenite fraction from the measured length change were compiled using Matlab.

## 4. Results and discussion

### 4.1. Thermodynamic analysis and SEM observation

As it is not clear whether the substitutional alloying elements diffuse during intercritical annealing [26] or not [24], it is assumed here that ortho-equilibrium, rather than para-equilibrium, pertains. The MTDData-calculated temperature dependence of the volume fractions and the carbon concentration in austenite for the 0.16C-1.5Mn-0.4Si TRIP steel is shown in Fig. 1. One

can see that when the temperature is below the  $Ae_1$  temperature (684°C), the material consists of 97.63 wt% of ferrite ( $\alpha$ ) and 2.37 wt% of cementite ( $\theta$ ). As the temperature increases to above the  $Ae_1$  temperature, both cementite and ferrite start to transform to austenite ( $\gamma$ ) until the  $Ae'_1$  temperature (698°C) is reached, at which the cementite is completely decomposed. In this temperature range, the carbon concentration ( $C^\gamma$ , in wt%) in austenite slightly increases as a function of temperature, from 0.61% to 0.65%. When the temperature is above the  $Ae'_1$  temperature, the ferrite further transforms to austenite and  $C^\gamma$  decreases as a function of temperature, until the  $Ae_3$  temperature (818°C). Since the equilibrium austenite fraction can be regarded as the upper-limit of austenite fraction during intercritical annealing, the thermodynamic data are helpful to understand the calculated results from the dilatometric data.

SEM observations of interruptedly quenched samples provide another means to determine the austenite

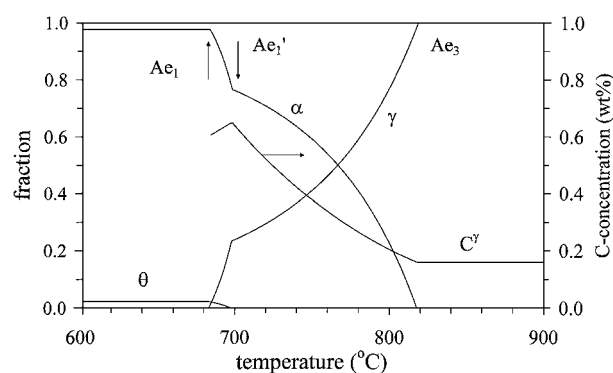


Figure 1 The temperature dependence of volume fractions and carbon concentration in austenite ( $C^\gamma$ , in wt%) in a 0.16C-1.5Mn-0.4Si steel, calculated from ortho-equilibrium thermodynamic analysis.

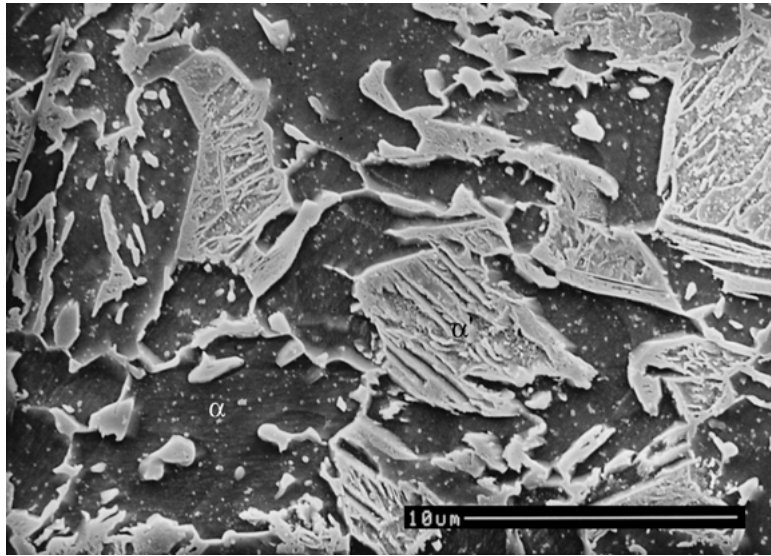


Figure 2 One of the SEM images for the samples quenched from 800°C ( $\alpha$ : ferrite;  $\alpha'$ : martensite).

volume fraction at the end of intercritical annealing. Fig. 2 shows one example of such SEM images. By analysis of a substantial number of images, the average austenite fraction is determined to be  $0.43 \pm 0.04$  and  $0.66 \pm 0.04$ , after intercritical annealing at 750°C and 800°C, respectively. The variation of the results may arise from the inhomogeneity of the materials.

#### 4.2. Dilatometry curves

The length change ( $\Delta l$ ) as a function of time and temperature as recorded in dilatometric experiments is shown in Fig. 3 for the samples annealed at 750°C, 800°C and 900°C, respectively. One can see that the expansion before (for all curves) and after transformation (only for the 900°C curve) is nearly linear, from which the expansion coefficient was derived ( $24.4 \times 10^{-6}/^\circ\text{C}$  for austenite and  $17.5 \times 10^{-6}/^\circ\text{C}$  for ferrite, respectively). One can also see that the end of the cementite decomposition is clearly indicated by an inflexion of the curve. The  $Ac_1$ ,  $Ac_1'$  and  $Ac_3$  (only from the 900°C curve) temperatures at 100°C/min. are determined to be 737°C, 754°C and 847°C, respectively, which are about 53°C, 55°C and 29°C higher than the corresponding equilibrium temperatures. The smaller difference for the end temperature is due to the effect of the transformation kinetics.

The isothermal holding at 750°C and 800°C for 10 min. leads to an approximately 6  $\mu\text{m}$  and 10  $\mu\text{m}$  decrease of the  $\Delta l$  value (Fig. 3b), and most of the length change is taking place within the first 3 min (Fig. 3a). The absolute values of the length change at 750°C are higher than that at 800°C (Fig. 3a). This is due to the fact that there is more austenite formed at 800°C and that the amount of existing phases has a larger effect on the length change than the temperature rise. At the end of isothermal holding at 750°C and 900°C, one can see a jump of the curve (Fig. 3a), which is an experimental artefact by the sudden introduction of gas into the sample chamber to quench the sample.

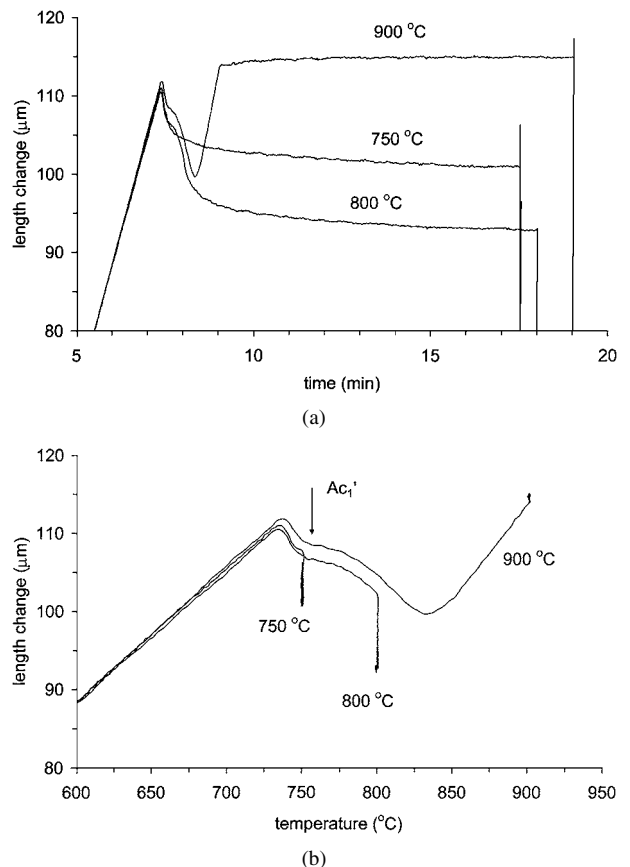


Figure 3 Length change ( $\Delta l$ ) as a function of (a) time, and (b) temperature, during intercritical annealing at 750°C and 800°C and during heating to the austenite region at 900°C, followed by isothermal holding for 10 min.

#### 4.3. Calculations based on lattice parameters

According to the evaluation method described in Section 2, the fractions of the various phases and the carbon concentration in austenite can be calculated. The lattice parameters used for the calculations are listed in Table I. Lattice parameters of ferrite and cementite determined by various authors appear to show a relatively small variation. This is due to the fact that

TABLE I The effect of temperature ( $T$ , in  $^{\circ}\text{C}$ ) and carbon content (only for austenite, in wt%) on the lattice parameters of ferrite and austenite (in  $\text{\AA}$ ). For cementite the volume of the unit cell (in  $\text{\AA}^3$ ) is given by the present authors based on Fig. 3d in reference [16]

| Phase     | Relation   | Ref. |
|-----------|--|------|
| Austenite | $a^{\gamma} = (3.6306 + 7.8 \times 10^{-3} \times \xi)[1 + (24.9 - 0.51 \times \xi) \times 10^{-6} \times (T - 723)]$<br>where $\xi = 4.650 \times C^{\gamma} / (3.650 \times C^{\gamma} + 100)$ | [17] |
| Ferrite   | $a^{\alpha} = 2.8863[1 + 17.5 \times 10^{-6} \times (T - 527)]$  | [17] |
| Cementite | $a^{\theta} b^{\theta} c^{\theta} = 153.85 + 0.00818 \times T$   | [16] |

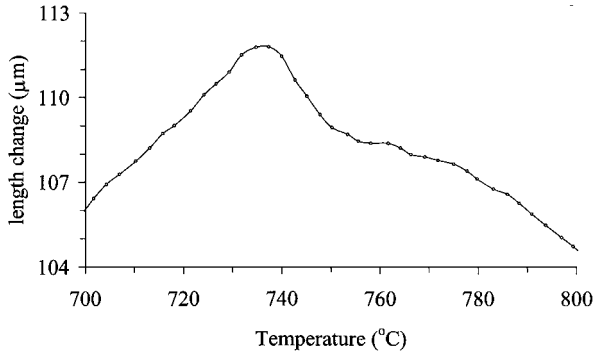
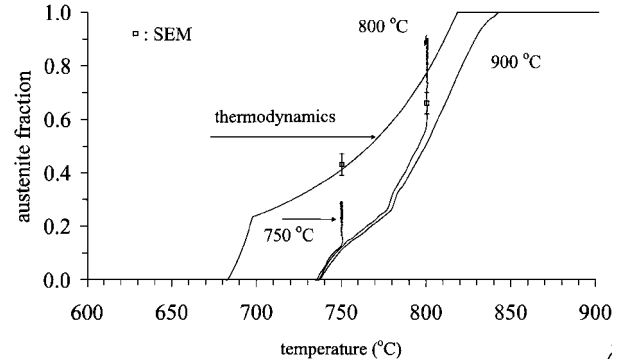


Figure 4 Comparison of measured (line) and calculated (circles) length change for the 900 $^{\circ}\text{C}$  curve.

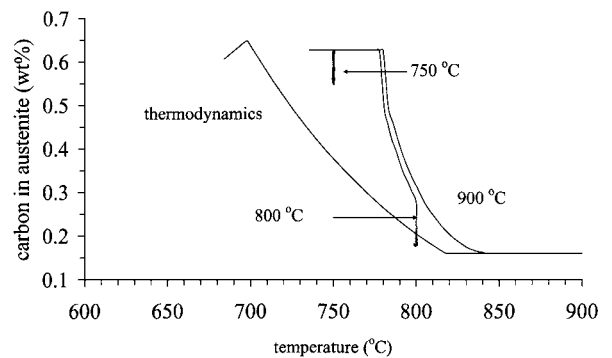
the lattice parameters of ferrite and cementite are not significantly influenced by carbon concentration, as indicated in Equation 4. However, significant discrepancies exist concerning the austenite lattice parameter [17–22]. In the present work, Onink *et al.*'s data [17] is used since using these data the  $\kappa^{\gamma}$  value is very close to 1 ( $\kappa^{\gamma} = 0.9997$ ), which agrees with the opinion of other authors [27] that Onink *et al.*'s data are the most reliable.

In the calculations, only two other experimental data besides the dilatometry curve, the starting and finishing austenite transformation temperatures ( $Ac_1$  and  $Ac_3$  temperatures), are required as input. For the calculation of the 750 $^{\circ}\text{C}$  and 800 $^{\circ}\text{C}$  curves, the scaling factor for austenite ( $\kappa^{\gamma}$ ) is taken from the 900 $^{\circ}\text{C}$  curve. The transition point from the three-phase region to the two-phase region, i.e. the  $Ac_1'$  temperature, is determined when the product of  $C^{\gamma}$  and  $f^{\gamma}$  equals  $C_0$ . Fig. 4 compares the measured length change with the calculated length change for the 900 $^{\circ}\text{C}$  curve, as an example, and one can see that the difference between these two length changes is negligible, indicating that the solution is found successfully in the iterative analysis.

The calculated temperature dependence of the austenite fraction and the carbon concentration for the 750 $^{\circ}\text{C}$ , 800 $^{\circ}\text{C}$  and 900 $^{\circ}\text{C}$  curves are shown in Fig. 5. From the final  $C^{\gamma}$  or  $f^{\gamma}$  value, one can see that isothermal holding at 750 $^{\circ}\text{C}$ , which is below the  $Ac_1'$  temperature, results in a complete decomposition of cementite. This is understandable since 750 $^{\circ}\text{C}$  is already above the equilibrium  $Ae_1'$  temperature (698 $^{\circ}\text{C}$ ). The final carbon concentration in austenite and the austenite fraction after isothermal holding at 750 $^{\circ}\text{C}$  is 0.57 wt% and 0.28, respectively. The austenite fraction is smaller than the equilibrium value (0.41) at 750 $^{\circ}\text{C}$  and the concentration is higher than the equilibrium value (0.38 wt%), indicating that the equilibrium is not reached yet. The calculated results also indicate that most of the austenite fraction is formed due to the cementite decomposition,



(a)



(b)

Figure 5 The calculated austenite volume fraction (a) and carbon concentration in austenite, (b) from the dilatometric data and from the thermodynamics, as a function of temperature.

i.e.  $\alpha + \theta \rightarrow \gamma$ , and only a small amount of austenite formed due to the  $\alpha \rightarrow \gamma$  transformation, judged from the transition point ( $Ac_1'$ ) where  $C^{\gamma} \cdot f^{\gamma} = C_0$ . The calculated results of the 800 $^{\circ}\text{C}$  curve show that the final austenite fraction after isothermal holding is 0.89, higher than the equilibrium value (0.78) and the fraction from the SEM observation (0.66). The calculated  $Ac_1'$  temperature from the 800 $^{\circ}\text{C}$  and 900 $^{\circ}\text{C}$  data is about 780 $^{\circ}\text{C}$ , which is 25 $^{\circ}\text{C}$  higher than the one from the experimental curve (see Fig. 3b). These inconsistencies are discussed in the following section.

#### 4.4. Discussion

In order to obtain the austenite fraction ( $f^{\gamma}$ ), three methods were applied: ortho-equilibrium thermodynamic analysis, SEM observations and the proposed evaluation method based on lattice parameters and dilatometry data. Table II summarizes  $f^{\gamma}$  and  $C^{\gamma}$  at the end of intercritical annealing at 750 $^{\circ}\text{C}$  and 800 $^{\circ}\text{C}$ , and one can see that the difference between the values from different methods is significant. As described in the previous sections, the austenite fraction after annealing at 750 $^{\circ}\text{C}$  calculated using the proposed method is

TABLE II Summary of austenite fraction,  $f^\gamma$ , and carbon concentration,  $C^\gamma$ , at the end of intercritical annealing determined by various methods

|                 | $f^\gamma$ |       | $C^\gamma$ |          |
|-----------------|------------|-------|------------|----------|
|                 | 750°C      | 800°C | 750°C      | 800°C    |
| Proposed method | 0.28       | 0.87  | 0.57 wt%   | 0.18 wt% |
| Thermodynamics  | 0.41       | 0.78  | 0.38 wt%   | 0.20 wt% |
| SEM             | 0.43       | 0.66  | –          | –        |

lower than the fraction given by the other two methods. Moreover the SEM-determined austenite fraction is slightly higher than the equilibrium value. However, the austenite fraction after 800°C annealing from the proposed method is higher than the equilibrium value, which is less likely. In addition to the drawbacks of studying down-quenched samples, the inconsistencies may arise from the following reasons.

From the viewpoint of thermodynamics calculation, the controversy about ortho-equilibrium or para-equilibrium is not clarified. However, the discrepancy between results from these two assumptions would decrease as the temperature increases. For instance, the manganese content in austenite is 2.39 wt% at 750°C and 1.72 wt% at 800°C under ortho-equilibrium assumption, as compared to 1.5 wt% under para-equilibrium assumption. From this, one can see that the controversy would not be the major cause of the inconsistencies. As to the proposed method, more accurate results would be obtained if the following measures were taken. Firstly, one can see that the method hinges on the point whether the lattice parameters of existing phases are exactly known. The present paper approached the problem by means of using literature data on lattice parameters from similar, but not identical, materials and introducing a scaling factor to account for the difference between experimentally measured and calculated values. If the lattice parameters can be measured at the temperatures investigated, the fraction and the concentration can be obtained more accurately and the calculation is mathematically simpler [13], although it would request additional experiments. Secondly, both crystallographic and microstructural isotropy is assumed in this paper, which is not exactly true for the hot-rolled steels and usually even more serious in cold-rolled steels [8, 28]. The calculation would be improved if the texture and initial microstructure could be taken into account. Thirdly, during the development of Equation 1, the square and cubic term of  $\Delta l/l_0$  were neglected, which would influence the accuracy to some extent since the magnitude of  $\Delta l/l_0$  is around 0.01. If only the cubic term is omitted, the accuracy is expected to be a bit higher although it is mathematically more complicated.

Compared with the SEM method or thermodynamic calculations, the calculation proposed in this paper is based on the consideration of its physical background. In spite of the inconsistencies among the results from various methods, the advantage is obvious since it gives an *in situ* description of the transformation kinetics, for instance, the determination of the time when the cementite is completely dissolved. The results are bene-

ficial in the design of processing routes in TRIP steels, particularly in the case that the intercritical annealing temperature is close to the  $A_{c1}$  temperature or/and the annealing time is short.

## 5. Conclusions

In this paper, the subject of quantitative determination of the austenite fraction and the carbon concentration in austenite during intercritical annealing from dilatometric data has been investigated. Based on the lattice parameters of existing phases and introduction of the scaling factor, an evaluation formulation has been proposed, in which two different cases during intercritical annealing were taken into account. One case concerns the three phase region (ferrite, cementite and austenite) just above the  $A_{c1}$  temperature, in which the carbon concentration in austenite is assumed to be constant. Another case is the two-phase region (ferrite and austenite) with a variable carbon concentration in austenite. The proposed method was applied to the dilatometric data in a 0.16C-1.5Mn-0.4Si TRIP multiphase steel annealed at 750°C (a three phase microstructure) and 800°C (a two-phase microstructure) with help of the data of heating up to 900°C. The calculated results show a reasonable temperature dependence of the austenite fraction and the carbon concentration during intercritical annealing. Comparison of the new results with the results from the microscopic observation as well as with those from the ortho-equilibrium thermodynamic calculation showed a considerable intertest variation.

## References

1. Y. SAKUMA, O. MATSUMURA and O. AKISUE, *ISIJ Int.* **31** (1991) 1348.
2. H. C. CHEN, H. ERA and M. SHIMIZU, *Metall. Trans.* **20A** (1989) 437.
3. O. MATSUMURA, Y. SAKUMA and H. TAKECHI, *Trans. ISIJ* **27** (1987) 570.
4. P. JACQUES, T. CATLIN, N. GEERLOFS, T. KOP, S. VAN DER ZWAAG and F. DELANNAY, *Mat. Sci. Eng.* **273-275A** (1999) 475.
5. M. DE MEYER, D. VANDERSCHUEREN and B. C. DE COOMAN, in 41st MWSP Conf. Proc. ISS. Vol. XXXVII (1999) p. 265.
6. L. ZHAO, N. H. VAN DIJK, E. BRÜCK, J. SIETSMA and S. VAN DER ZWAAG, *Mat. Sci. Eng.* **313A** (2001) 145.
7. L. ZHAO, J. SIETSMA and S. VAN DER ZWAAG, in *Euromat 99 Vol. 7 Steels and Materials for Power Plants*, edited by P. Neumann *et al.* (Wiley-Vch, Weinheim, 2000) p. 77.
8. J. Y. YANG and H. K. D. H. BHADSHIA, *Mat. Sci. Eng.* **118A** (1989) 155.
9. R. C. DYKHUIZEN, C. V. ROBINO and G. A. KNOROVSKY, *Metall. Mater. Trans.* **30B** (1999) 107.
10. T. A. KOP, J. SIETSMA and S. VAN DER ZWAAG, *J. Mater. Sci.* **36** (2001) 519.
11. C. QIU and S. VAN DER ZWAAG, *Steel Res.* **88** (1997) 32.
12. H. K. D. H. BHADSHIA, *J. de Physique* **C4** (1982) 443.
13. R. C. REED, T. AKBAY, Z. SHEN, J. M. ROBINSON and J. H. ROOT, *Mater. Sci. Eng.* **256A** (1998) 152.
14. C. M. LI, F. SOMMER and E. J. MITTEMEIJER, *Z. Metallkd.* **91** (2000) 5.
15. H. STUART and N. RIDLEY, *J. Iron Steel Inst.* (1966) 711.
16. R. C. REED and J. H. ROOT, *Scripta Mater.* **38** (1998) 95.

17. M. ONINK, C. M. BRAKMAN, F. D. TICHELAAAR, E. J. MITTEMEIJER, S. VAN DER ZWAAG, J. H. ROOT and N. B. KONYER, *Scripta Metall. Mater.* **29** (1993) 1011.
18. D. J. DYSON and B. HOLMES, *J. Iron Steel Inst.* (1970) 469.
19. C. S. ROBERT, *J. Metals* **5** (1953) 203.
20. M. X. ZHANG and P. M. KELLY, *Mater. Charact.* **40** (1998) 159.
21. R. C. RUHL and M. COHEN, *Trans. AIME* **245** (1969) 241.
22. N. RIDLEY, H. STUART and L. ZWELL, *ibid.* **245** (1969) 1834.
23. E. KREYSZIG, in "Advanced Engineering Mathematics," 7th ed. (John Wiley & Sons, New York, 1993) p. 929.
24. P. JACQUES, X. CORNET, PH. HARLET, J. LADRIÈRE and F. DELANNAY, *Metal. Mater. Trans.* **29A** (1998) 2383.
25. E. GIRAULT, P. JACQUES, PH. HARLET, K. MOLS, J. VAN HUMBEECK, E. AERNOUDT and F. DELANNAY, *Mater. Charact.* **40** (1998) 111.
26. S. SUN and M. PUGH, *Mater. Sci. Eng.* **276A** (2000) 167.
27. M. DE MEYER, D. VANDERSCHUEREN, K. DE BLAUWE and B. C. DE COOMAN, in 41st MWSP Conf. Proc. ISS. Vol. XXXVII (1999) p. 483.
28. T. A. KOP, J. SIETSMA and S. VAN DER ZWAAG, *Mat. Sci. & Tech.* **17** (2001) 1569.

*Received 4 April  
and accepted 29 November 2001*